Journal of Ceramic Processing Research. Vol. 16, No. 1, pp. 18~23 (2015)

JOURNAL OF
Ceramic
Processing Research

Effects of Ti nonstoichiometry on microstructure, dielectric, ferroelectric and piezoelectric properties of $(Na_{0.54}Bi_{0.5})_{0.94}Ba_{0.06}Ti_{1+x}O_3$ lead-free ceramics

Xu-mei Zhao, Xiao-ming Chen*, Jian Wang, Xiao-xia Liang, Jian-ping Zhou and Peng Liu
College of Physics and Information Technology, Shaanxi Normal University, Xi'an 710119, P. R. China

The lead-free ceramics $(Na_{0.54}Bi_{0.5})_{0.94}Ba_{0.06}Ti_{1+x}O_3$ with x = –0.02, 0, 0.02, and 0.04 were prepared by a solid-state reaction method. Effects of Ti^{4+} nonstoichiometry on crystallite structure, microstructure, dielectric, ferroelectric and piezoelectric properties were studied. The ceramics with x = –0.02 and 0 exhibit typical diffraction peaks of perovskite structure. A secondary phase appears in the ceramics with x = 0.02 and 0.04. The rhombohedral-tetragonal morphotropic phase boundary exists in all samples, and the relative amount of the tetragonal phase changes with the increase in the Ti^{4+} amount from deficiency to excess. Grain sizes and shape of the ceramics are unaffected by changes in Ti^{4+} nonstoichiometry. But, dielectric, ferroelectric and piezoelectric properties of the ceramics are close related to the Ti^{4+} amounts. Compared with the ceramic with x = 0, the ceramics with the Ti^{4+} nonstoichiometry have higher depolarization temperature, lower maximum dielectric constant, decreased piezoelectric constant and ferroelectric properties.

Key words: Bismuth sodium titanate, Structure, Dielectric properties, Ferroelectric properties, Piezoelectric properties.

Introduction

Piezoelectric ceramics are widely used in ultrasonic transducer, filter, piezoelectric transformer, piezoelectric buzzer device, and so on. Synthesis, application and waste reprocessing of lead -based ceramics are harmful to environment. Therefore, lead-free ceramics have attracted considerable attention. Among lead-free ceramics, bismuth sodium titanate ($Na_{0.5}Bi_{0.5}TiO_3$, BNT) has been considered to be a promising candidate material owing to its high Curie temperature and strong ferroelectric [1]. Great efforts have been devoted to studying BNT-based solid solutions [2-14]. Among them, $(Na_{0.54}Bi_{0.5})_{1-x}Ba_xTiO_3$ near x = 0.06 shows excellent electrical properties due to the existence of a rhombohedral-tetragonal morphotropic phase boundary (MPB) [6-14].

Nonstoichiometry of elements can affect structure and electrical properties of BNT -based ceramics obviously [15-28]. Because of the volatility of Na^+ and Bi^{3+}, most studies have focused on effect of deviation of Na^+ and Bi^{3+} from stoichiometry on electrical properties of BNT -based ceramics [19-26]. Sung et al. reported that the BNT ceramics with Bi excess have higher piezoelectric coefficient and lower depolarization temperature compared with those with Bi deficiency; however, effect of Na nonstoichiometry is different from that of Bi nonstoichiometry [19, 20]. Park et al. revealed that volatilization of Bi^{3+} during the process of crystal growth has an important effect on structure and electrical properties of the BNT crystals [21, 22]. Zuo et al. studied the influence of A-site nonstoichiometry on microstructure and electrical properties of BNT -based ceramics and found that the excess of A-site $(Bi_{0.5}Na_{0.5})^{2+}$ can effectively enhance electrical properties [23]. Addition or lack of $(Na_{0.5}Bi_{0.5})^{2+}$ in A-site can also improve piezoelectric properties of the $(Na_{0.5}Bi_{0.5})_{0.92}Ba_{0.08}TiO_3$ ceramics [24]. Xu et al. also reported that electrical properties of the 0.93BNT-0.07$BaTiO_3$ ceramics are associated with the deficiency and excess of Bi^{3+} in the ceramics [25, 26]. In our previous work, we have studied effect of Na^+ nonstoichiometry on microstructure, dielectric and ferroelectric properties of the $(Na_xBi_{0.5})_{0.94}Ba_{0.06}TiO_3$ ceramics and found that the ceramic with excess Na^+ (x = 0.54) shows excellent electrical properties [27]. As far as we know, many studies have explored influence of Bi^{3+} and Na^+ nonstoichiometry on structure and electrical properties of BNT -based ceramics; however, few reports about effects of Ti^{4+} nonstoichiometry are available [28]. Naderer et al. reported the influence of Ti-nonstoichiometry in $Bi_{0.5}Na_{0.5}TiO_3$ and found that the temperature -dependent electrical properties are close related to the content of Ti^{4+} [28]. To our knowledge, effects of Ti^{4+} nonstoichiometry on structure and electrical properties of BNT -based ceramics with the MPB have not been clarified. In the present work, $(Na_{0.54}Bi_{0.5})_{0.94}Ba_{0.06}Ti_{1+x}O_3$ lead-free ceramics with the MPB were prepared via a solid state reaction method. Effects of Ti^{4+} nonstoichiometry on crystallite structure, microstructure, dielectric, ferroelectric and piezoelectric properties of the ceramics were studied in detail.

*Corresponding author:
Tel : +86-29-81530750
Fax: +86-29-81530750
E-mail: xmchen-snnu@163.com

Materials and Experimental Methods

The $(Na_{0.54}Bi_{0.5})_{0.94}Ba_{0.06}Ti_{1+x}O_3$ (BNBT-xTi, x = –0.02, 0, 0.02, and 0.04) lead-free ceramics were prepared via a conventional solid state reaction method. Starting materials are $BaCO_3$ (99%), TiO_2 (99.99%), Na_2CO_3 (99.8%) and Bi_2O_3 (98.9%) powders. All raw powder were baked at 100 °C for 24 h to remove water and immediately weighed according to the chemical formula. The powders were put in agate vials with agate balls and milled for 24 h using alcohol as a medium. After drying, the milled powders were calcined at 920 °C for 3 h. The calcined powders were milled again for 12 h and then pulverized with approximately 5 wt% polyvinyl alcohol. Pellets of 11.5 mm in diameter and approximately 1.5 mm in thickness were pressed under a uniaxial pressure of 300 MPa and burned out the binder at 500 °C for 2 h. Samples were sintered at 1170 °C for 3 h. Heating and cooling rates were 3 °C/min. In order to prevent the volatility of Bi^{3+} and Na^+, the pellets were embedded in the corresponding powders and put in covered alumina crucibles.

Relative densities of the ceramics were calculated according to $\rho_r = \rho_b/\rho_t$, where ρ_b and ρ_t are the bulk density of the sintered ceramics obtained by Archimedes method, and the theoretical one, respectively. The theoretical density (5.98 g/cm^3) of $(Na_{0.5}Bi_{0.5})_{0.94}Ba_{0.06}TiO_3$ was roughly used for all compositions. X-ray diffraction (XRD, Rigaku D/Max 2550) in a step mode using a Cu K_α radiation was used for the identification of phase compositions. The measurements were made at 40 kV and 100 mA with a step size of 0.02 ° in the 2θ range of 20-70 °. Additionally, in order to examine the XRD peaks around 46.5 ° more precisely, data were collected in the 2q ranges of 45.5-47.5 ° with a scanning step of 0.006 °. Microstructure was observed by means of a scanning electron microscope (SEM, Hitachi High-Tech, Ibaraki-ken, TM-3000). Average grain size was determined by means of the linear intercept method. To characterize electrical properties of the samples, external surfaces of the ceramics were mechanically ground and polished using fine-grained emery paper under cold-water circulation. Then, silver electrodes were coated and fired at 650 °C for 40 min. Dielectric measurement was performed with a precision LCR meter (Agilent E4980A) from room temperature to 550 °C at 3 °C/min. The samples were poled in a silicon oil bath at room temperature under an electric field of 3 kV/mm for 15 min. The piezoelectric constant d_{33} of the ceramics was measured using a quasistatic d_{33} meter (ZJ-4A Institute of Acoustics, Chinese Academy of Sciences, Beijing, China) based on the Berlincourt method at 110 Hz. The electromechanical coupling (K_p) and mechanical quality factor (Q_m) were calculated by means of the resonance and anti-resonance method [29]. Ferroelectric hysteresis loops were measured at 50 Hz and room temperature in silicon oil with a radiant precision workstation ferroelectric testing system (Radiant Technologies. Inc.).

Results and Discussion

Figure 1 shows XRD patterns of the BNBT-xTi lead-free ceramics with various Ti^{4+} amounts. XRD data shows that the samples with x = –0.02 and 0 form pure perovskite structure. But, a secondary phase appears in the ceramics with x = 0.02 and 0.04, which should be caused by the excess Ti^{4+}. A rhombohedral - tetragonal MPB exists in the composition of $(Na_{0.5}Bi_{0.5})_{1-x}Ba_xTiO_3$ near x = 0.06 [30], so that the XRD peaks around 46.5 ° are characterized with (002) and (200) peaks corresponding to tetragonal phase and (200) peaks corresponding to rhombohedral phase [31]. Further XRD analysis for the BNBT-xTi ceramics performed in the 2θ ranges of 45.5-47.5 ° is shown in Fig. 2. The peaks in the 2θ range of 45.5-47.5 ° were fitted into $(002)_T$, $(200)_T$ and $(200)_R$ peaks for all ceramics, where T and R denote tetragonal and rhombohedral phase, respectively. The percentages of the tetragonal phase T% were determined from the equation of T%

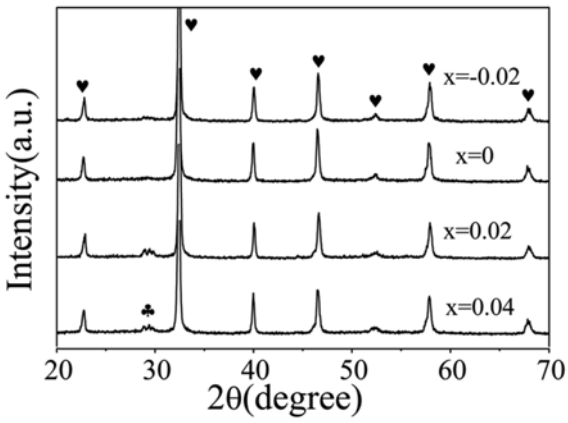

Fig. 1. XRD patterns of the ceramics with various x, in which the symbols ♥ and ♣ demonstrate perovskite structure and secondary phase, respectively.

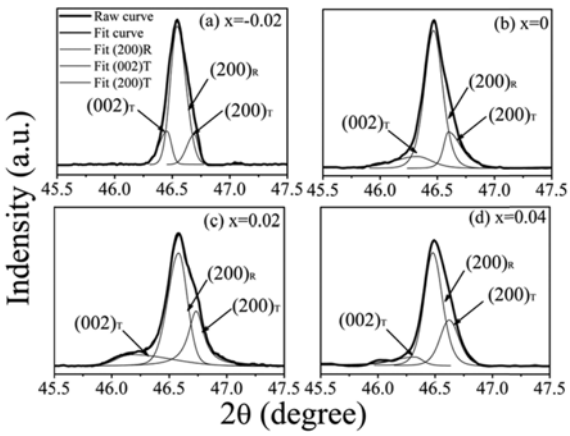

Fig. 2. XRD fitting patterns of the ceramics in the 2θ range of 45.5-47.5 °: (a) x = –0.02, (b) x = 0, (c) x = 0.02, (d) x = 0.04.

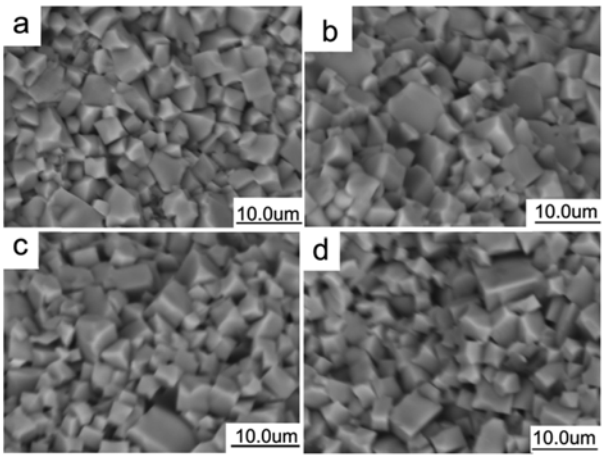

Fig. 3. SEM images of the fractures of the ceramics: (a) x = –0.02, (b) x = 0, (c) x = 0.02, (d) x = 0.04.

Table 1. Average grain size, relative density, relative percentage of the tetragonal phase (T%), dielectric, ferroelectric and piezoelectric properties of the ceramics.

	x = –0.02	x = 0	x = 0.02	x = 0.04
Average grain size (μm)	1.0	1.1	1.1	1.1
Relative density (%)	93.4	93.8	94.1	93
T%	26	30	44	35
T_d (°C, 10 kHz)	89	82	87	84
T_m (°C, 100 kHz)	263	272	274	274
ε_m (100 kHz)	6510	7207	6122	6712
tanδ (100 kHz)	0.0690	0.0410	0.0548	0.0454
P_m (μC/cm^2, 45 kV/cm)	25.4	27.4	26.1	/
P_r (μC/cm^2, 45 kV/cm)	31.7	32.4	28.2	/
E_c (kV/cm, 45 kV/cm)	29.6	28.9	28.2	/
K_p	0.3288	0.3442	0.2637	0.2408
Q_m	12.86	23.24	25.20	37.83
d_{33} (pC/N)	56	116	80	81

$= (Area_{(200)T} + Area_{(002)T})/(Area_{(200)T} + Area_{(002)T} + Area_{(200)R})$. The values of T% were determined to be approximately 26%, 30%, 44%, 35% for the ceramics with x = –0.02, 0, 0.02, and 0.04, respectively. The ceramic with the deficient Ti^{4+} shows a decrease in the T%, while the excess Ti^{4+} causes an increase in the T%.

Figure 3 shows SEM images of the fractures of the ceramics with various Ti^{4+} amounts. The ceramics have fine microstructures with cube-shaped grains. Almost no pores are observed in the ceramics. The sizes of grains in all ceramics are about 1 μm (Table 1). The ceramics with different Ti^{4+} amounts show rather similar grain size, indicating that the Ti^{4+} nonstoichiometry produces an ignorable effect on grain size.

Figure 4 shows variation in dielectric constant (ε_r) of the poled ceramics with various Ti^{4+} amounts as a function of temperature (T). All ceramics show two dielectric anomalies in the ε_r-T curves. The dielectric anomaly on the higher temperature side is denoted by T_m,

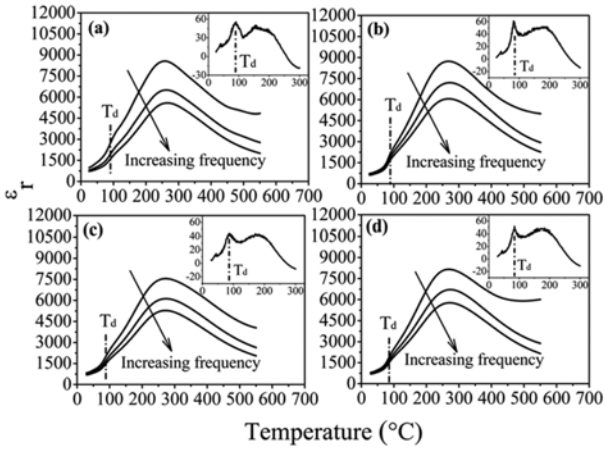

Fig. 4. Dielectric constant (ε_r) of the poled ceramics with various x vs. temperature at frequencies of 10 kHz, 100 kHz and 1 MHz. The insets show the first derivative curves of the ε_r at frequencies of 10 kHz.

at which the dielectric constant reaches the maximum (ε_m). At temperatures higher than T_m, ε_r decreases as the temperature increases. The anomaly on the lower temperature side is related to the depolarization temperature T_d [32]. For BNT -based ceramics, the determination of T_d and interpretation of the anomaly around T_d are different by different authors [32]. Here, we determine the T_d values as the temperatures at which ε_r increases sharply. The T_d values were obtained from the temperatures corresponding to the maximum values of first derivative of ε_r (as shown in the insets of Fig. 4). The anomaly around T_d is traditionally attributed to the phase transition between a ferroelectric phase and an "anti-ferroelectric phase", due to the appearance of double hysteresis loops above T_d [33]. However, double hysteresis loops may also be related to other factors, such as macro-micro domain switching [34], interactions between polar and non-polar regions [35], and subtle modulation of spontaneous polarization [36]. Thus, a so-called "intermediate phase" is suggested above T_d and the dielectric anomaly near T_d is assumed to be caused by the phase transition from the ferroelectric phase to the "intermediate phase" [37, 38]. The strong frequency dispersion above T_d is also found, which suggests a relaxor characteristic. Ma et al. observed that nanodomains with short range order exist in (1-x) BNT-xBT with $0.06 \le x \le 0.11$ and proposed a new term "relaxor anti-ferroelectric" to describe this kind of ceramics [39]. The values of ε_m, T_d, and T_m are shown in Table 1. The ceramic with x = 0 shows the highest ε_m value. Both the excess and deficient Ti^{4+} cause a decrease in the ε_m values. The T_d values of the ceramics with x = –0.02, 0, 0.02 and 0.04 are 89 °C, 82 °C, 87 °C and 84 °C respectively. The ceramics with Ti^{4+} nonstoichiometry have increased T_d values compared with the ceramic with x = 0. Compared with the T_m value of the ceramic with x = 0, that of the ceramic with deficient Ti^{4+} decreases, while that of the ceramics with

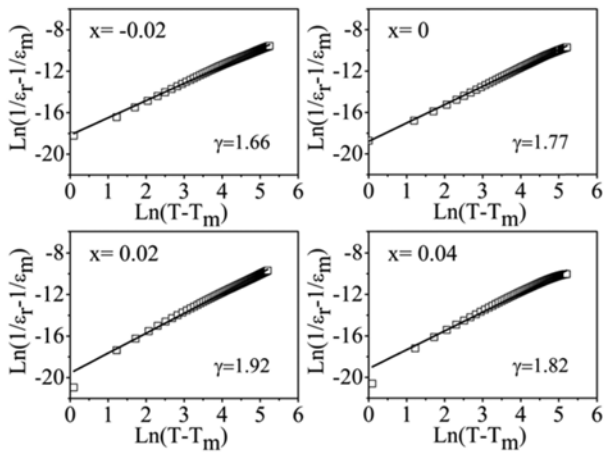

Fig. 5. Plots of $Ln(1/\varepsilon_r-1/\varepsilon_m)$ vs. $Ln(T-T_m)$ of the ceramics with various x at 10 kHz. The symbols denote experimental data, while the solid lines denote the least-square fitting curves to the modified Curie-Weiss law.

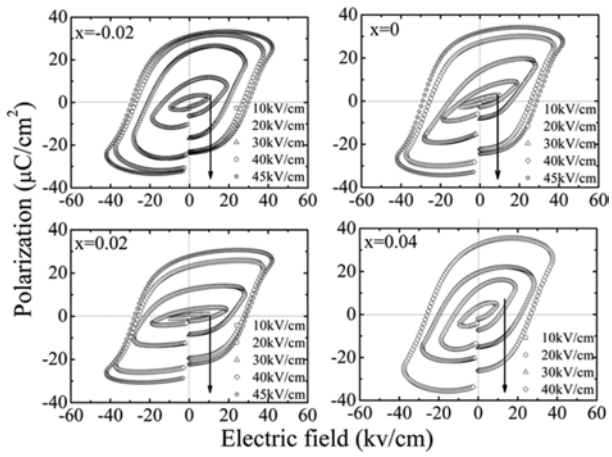

Fig. 6. P-E loops of the ceramics with various x under different driving electric fields.

excess Ti^{4+} increases slightly. Phase transition temperature is related to many factors. Uchino et al. found that Curie temperature of $BaTiO_3$ is affected by grain size as the size is less than 200 nm [40]. Here, the ceramics with different Ti^{4+} amounts show rather similar mean grain size (about 1 μm, far larger than 200 nm). It is unlikely that grain size is responsible for the variation in T_m. Fisher et al. reported that a secondary phase can cause a change in T_m [41]. Here, the secondary phase exists in the samples with x = 0.02 and 0.04. So, the change in the T_m for the ceramics with excess Ti^{4+} is associated with the existence of the secondary phase. In our previous work, we found that the relative amount of the tetragonal phase and defect concentration can also affect T_m values and dielectric constant of the BNT-based ceramics [27]. Here, the relative amount of the tetragonal phase changes with the change in Ti^{4+} contents. In addition, cation vacancy concentration and oxygen vacancy concentration may change in the ceramics with different Ti^{4+} amounts. All these factors can affect the values of T_m and ε_m.

The ε_r-T curves exhibit broad dielectric peaks and frequency dependency around T_m. The dielectric behaviors were further studied by fitting the results of temperature dependency of dielectric constant to the modified Curie-Weiss law, which is described as [42]: $1/\varepsilon_r-1/\varepsilon_m = (T-T_m)^\gamma/C'$, where ε_m is the maximum value of dielectric constant at phase transition temperature T_m, C' is Curie-like constant, and γ is the degree of diffuseness. γ is usually ranging from 1 for a normal ferroelectric to 2 for an ideal relaxor ferroelectric. Plots of $Ln(1/\varepsilon_r-1/\varepsilon_m)$ as a function of $Ln(T-T_m)$ for all samples at 10 kHz are shown in Fig. 5. All samples exhibit a linear characteristic. By least-square fitting the experimental data to the modified Curie-Weiss law, γ was obtained. The γ values of all samples are close to 2. All ceramics show the characteristic of diffuse phase transition.

Figure 6 shows polarization (P) of the ceramics with various Ti^{4+} amounts versus applied electric field (E) at 50 Hz and room temperature. In order to obtain the saturated polarization characterization, all ceramics were measured under different electric fields. For the ceramics with x = –0.02, 0 and 0.02, electric fields with E = 45 kV/cm can be applied. But, the same electric field cannot be applied to the ceramic with x = 0.04 because of high leakage currents. The remnant polarization (P_r), maximum polarization (P_m) and coercive field (E_c) of the samples are determined from the P-E loops and shown in Table 1. Compared with the ceramic with x = 0, the ceramics with Ti^{4+} nonstoichiometry demonstrate decreased P_r and P_m values. With increasing Ti^{4+} amount from deficiency to excess, E_c decreases slightly. The ceramic with x = 0 exhibits highest P_r and P_m of 32.4 μC/cm^2 and 27.4 μC/cm^2, respectively. The Ti^{4+} nonstoichiometry causes a decrease in the ferroelectric properties. In our previous work, we found that ferroelectric properties of the BNT -based ceramics are associated with grain size, A-site vacancies, and oxygen vacancies [43-44]. As grain size is about or less than 1 μm, the coupling between grain boundaries and domain walls becomes very strong [45]. The stronger the coupling is, the weaker the ferroelectric properties are because of the decrease in domain wall mobility and achievable domain alignment. Here, all ceramics show fine grains, which can decrease the ferroelectric properties. But, the ceramics with various Ti^{4+} amounts show rather similar grain sizes. So, it is reasonable to expect that the difference in ferroelectric properties among the ceramics with different Ti^{4+} amounts should precede to be associated with other factors. The structure of ABO_3-type perovskites can be viewed as a network of $[BO_6]$ oxygen octahedra, where the B-site cations are at the center of the sixfold coordinated octahedra and the A-site cations are in between. It is well known that the

spontaneous polarization in ABO_3-type perovskite ferroelectric mainly originates from the displacement of the B-site cations within the $[BO_6]$ octahedra. It can be expected that B-site vacancies are created in the ceramic with Ti^{4+} deficiency, which would reduce the number of active diploes per unit volume and result in a detrimental effect on the ferroelectric properties. For the ceramics with Ti^{4+} excess, the changes in the ferroelectric properties might be related to the existence of the secondary phase. The main piezoelectric, dielectric and ferroelectric properties of the ceramics with various Ti^{4+} amount are summarized in Table 1. The K_p and Q_m values change with the change in Ti^{4+} amounts. The ceramic with x = 0 shows the highest d_{33} value of 116 pC/N. Both the excess and deficient Ti^{4+} amounts cause a decrease in the piezoelectric constant.

Conclusions

Effects of Ti^{4+} nonstoichiometry on microstructure, dielectric, ferroelectric and piezoelectric properties of the $(Na_{0.54}Bi_{0.5})_{0.94}Ba_{0.06}Ti_{1+x}O_3$ lead-free ceramics were studied. The relative amounts of tetragonal phase for the ceramics with x = –0.02, 0, 0.02 and 0.04 are 26%, 30%, 44%, 35%, respectively. All ceramics show similar mean grain sizes. For the ceramics with Ti^{4+} nonstoichiometry, the depolarization temperature increases slightly and maximum dielectric constant decreases compared with the ceramic with x = 0. The ceramic with x = 0 exhibits highest P_r and P_m of 32.4 μC/cm^2 and 27.4 μC/cm^2, respectively. The Ti^{4+} nonstoichiometry causes a decrease in the polarization. With the increase in the Ti^{4+} amount from deficiency to excess, E_c decreases slightly. The sample with x = 0 shows the maximum value of d_{33} = 116 pC/N. Both the excess and deficient Ti^{4+} amounts result in a decrease in d_{33}.

Acknowledgments

This work was supported by the National Natural Science Foundation of China (No. 51372147), Shaanxi Province Science and Technology Foundation (No. 2012KJXX-30), Specialized Research Fund for the Doctoral Program of Higher Education (No. 20120202 110004), Fundamental Research Funds for the Central Universities (No. GK201305006, GK201401003), Innovation Funds of Graduate Programs, Shaanxi Normal University (Grant no. 2013CXS009) and National University Student Innovation Program (No. 201310718033).

References

1. G.A. Smolenskii, V.A. Isupov, A.I. Agranovskaya, N.N. Krainik, Sov. Phys. Solid. State 2 (1961) 2651-2654.
2. X.M. Chen, Y.W. Liao, H.P. Wang, L.J. Mao, D.Q. Xiao, J.G. Zhu, Q. Chen, J. Alloys. Compd. 493 (2010) 368-371.
3. E.V. Ramana, S.V. Suryanarayana, T.B. Sankaram, Solid State Sci. 12 (2010) 956-962.
4. H. Nagata, N. Koizumi, T. Takenaka, Key Eng. Mater. 169-170 (1999) 37-40.
5. W.C. Lee, C.Y. Huang, L.K. Tsao, Y.C. Wu, J. Alloys. Compd. 492 (2010) 307-312.
6. M. Cernea, E. Andronescu, R. Radu, F. Fochi, C. Galassi, J. Alloys. Compd. 490 (2010) 690-694.
7. T. Takenaka, K. Maruyama, K. Sakata, Jpn. J. Appl. Phys. 30 (1991) 2236-2239.
8. M.L. Liu, Y.F. Qu, D.A. Yang, J. Alloys. Compd. 503 (2010) 237-241.
9. S.T. Zhang, A.B. Kounga, W. Jo, C. Jamin, K. Seifert, T. Granzow, J. Rödel, D. Damjanovic, Adv. Mater. 21 (2009) 1-5.
10. J.E. Daniels, W. Jo, J. Rödel, V. Honkimäki, J.L. Jones, Acta Mater. 58 (2010) 2103-2111.
11. P. Fu, Z.J. Xu, R.Q. Chu, W. Li, G.Z. Zang, J.G. Hao, Mater. Sci. Eng. B 167 (2010) 161-166.
12. C.W. Tai, Y. Lereah, Appl. Phys. Lett. 95 (2009) 062901-062903.
13. Y.J. Dai, S.J. Zhang, T.R. Shrout, X.W. Zhang, J. Am. Ceram. Soc. 93 (2010) 1108-1113.
14. Y. Makiuchi, R. Aoyagi, Y. Hiruma, H. Nagata, T. Takenaka, Jpn. J. Appl. Phys. 44 (2005) 4350-4353.
15. Y. Kaneko, F. Azough, T. Kida, K. Ito, T. Shimada, T. Minemura, J. Am. Ceram. Soc. 95 (2012) 3928-3934.
16. R. J. Panlenere, R. N. Blumenthal, J. Am. Ceram. Soc. 54 (1971) 610-613.
17. X.X. Wang, S.W. Or, X.G. Tang, H.L.W. Chan, P.K. Choy, P.C.K. Liu, Solid State Commun. 134 (2005) 659-663.
18. X.X. Wang, X.G. Tang, K.W. Kwok, H.L.W. Chan, C.L. Choy, Appl. Phys. A 80 (2005) 1071-1075.
19. Y.S. Sung, J.M. Kim, J.H. Cho, T.K. Song, M.H. Kim, H.H. Chong, T.G. Park, D. Do, S.S. Kim, Appl. Phys. Lett. 96 (2010) 022901~1-022901-3.
20. Y.S. Sung, J.M. Kim, J.H. Cho, T.K. Song, M.H. Kim, T.G. Park, Appl. Phys. Lett. 98 (2011) 012902~1-012902-3.
21. S.E. Park, S.J. Chung, I.T. Kim, K.S. Hong, J. Am. Ceram. Soc. 77 (1994) 2641-2647.
22. S.E. Park, S.J. Chung, I.T. Kim, J. Am. Ceram. Soc. 79 (1996)1290-1296.
23. R.Z. Zuo, S. Su, Y. Wu, J. Fu, M. Wang, L.T. Li, Mater. Chem. Phys. 110 (2008) 311-315.
24. B.-J. Chu, D.-R. Chen, G.-R. Li, Q.-R. Yin, J. Eur. Ceram. Soc. 22 (2002) 2115-2121.
25. Q. Xu, Y.H. Huang, M. Chen, W. Chen, B.-H. Kim, B.-K. Ahn, J. Phys. Chem. Solids 69 (2008) 1996-2003.
26. Q. Xu, D.-P. Huang, M. Chen, W. Chen, H.-X. Liu, B.-H. Kim, J. Alloys. Compd. 471 (2009) 310-316.
27. X.M. Chen, H.Y. Ma, W.Y. Pan, M. Pang, P. Liu, Mater. Chem. Phys. 132 (2012) 368-374.
28. M. Naderer, T.Kainz, D. Schütz, K. Reichmann, J. Eur. Ceram. Soc. 34 (2014) 663-667.
29. M. Onoe, H. Jumonji, J. Acoust. Soc. Am. 41 (1967) 974-980.
30. X.P. Jiang, Y.Y. Zheng, F.L. Jiang, L.H. Liu, K.W. Kwok, H.L.W. Chan, Chin. Phys. Lett. 24 (2007) 3257-3259.
31. J.B. Lim, S.J. Zhang, J.H. Jeon, T.R. Shrout, J. Am. Ceram. Soc. 93 (2010) 1218-1220.
32. Y. Su, H.T. Chen, J.J. Li, A.K. Soh, G.J. Weng, J. Appl. Phys. 110 (2011) 084108~1-084108~6.
33. S.B. Vakhrushev, V.A. Isupov, B.E. Kvyatkovsky, N.M. Okuneva, I.P. Pronin, G.A. Smolensky, P.P. Syrnikov, Ferroelectrics 63 (1985) 153-160.
34. X.X. Wang, X.G. Tang, H.L.W. Chan, Appl. Phys. Lett. 85

(2004) 91-93.
35. J. Suchanicz, J. Kusz, H. Böhm, H. Duda, J.P. Mercurio, K. Konieczny, J. Eur. Ceram. Soc. 23 (2003) 1559-1564.
36. J.K. Lee, J.Y. Yi, K.S. Hong, J. Appl. Phys. 96 (2004) 1174-1177.
37. Y. Hiruma, H. Nagata, T. Takenaka, Jpn. J. Appl. Phys. 45 (2006) 7409-7412.
38. Y. Hiruma, Y. Imai, Y. Watanabe, H. Nagata, T. Takenaka, Appl. Phys. Lett. 92 (2008) 262904-1~262904-3.
39. C. Ma, X. Tan, E. Dul'kin, M. Roth, J. Appl. Phys. 108 (2010) 104105~1-104105~8.
40. J.G. Fisher, D. Rout, K.S. Moon, S.J.L. Kang, J. Alloys. Compd. 479 (2009) 467-472.
41. J.G. Fisher, D. Rout, K.S. Moon, S.J.L. Kang, Mater. Chem. Phys. 120 (2010) 263-271.
42. K. Uchino, S. Nomura, Ferroelectrics 44 (1982) 55-61.
43. X.M. Chen, X.X, Gong, T.N. Li, Y. He, P. Liu, J. Alloys. Compd. 507 (2010) 535-541.
44. X.M. Chen, W.Y. Pan, H.H. Tian, X.X. Gong, X.B. Bian, P. Liu, J. Alloys. Compd. 509 (2011) 1824-1829.
45. W.R. Buessem, L.E. Cross, A.K. Goswami, J. Am. Ceram. Soc. 49 (1966) 33-36.